MR based electric properties imaging for hyperthermia treatment planning and MR safety purposes

Balidemaj, E.

Publication date
2016

Document Version
Final published version

4 *In vivo* electric conductivity of cervical cancer patients based on B_1^+ maps at 3T MRI

This chapter is published as:
E. Balidemaj, P. de Boer, A.L.H.M.W. van Lier, R.F. Remis, L.J.A. Stalpers, G.H. Westerveld, A.J. Nederveen, C.A.T. van den Berg and J. Crezee, "In vivo electric conductivity of cervical cancer patients based on B_1^+ maps at 3T MRI," *Physics in Medicine and Biology*, Vol. 61, No. 4, pages 1596-1607, 2016

Abstract

Purpose: In vivo electric conductivity (σ) values of tissue are essential for accurate electromagnetic simulations and Specific Absorption Rate (SAR) assessment for applications such as thermal dose computations in hyperthermia. Currently used σ-values are mostly based on ex vivo measurements. In this study conductivity of human muscle, bladder content and cervical tumors are acquired non-invasively in vivo using MRI.
Methods: The conductivity of 20 cervical cancer patients was measured with the MR-based Electric Properties Tomography method on a standard 3T MRI system.
Results: The average in vivo σ-value of muscle is 14% higher than currently used in human simulation models. The σ-value of bladder content is an order magnitude higher than the value for bladder wall tissue that is used for the complete bladder in many models. Our findings are confirmed by various in vivo animal studies from the literature. In cervical tumors, the observed average conductivity was 13% higher than the literature value reported for cervical tissue.
Conclusions: Considerable deviations were found for electrical conductivity observed in this study and the commonly used values for SAR assessment, emphasizing the importance of acquiring the in vivo conductivity for more accurate SAR assessment in various applications.

4.1 Introduction

Accurate tissue electric properties (conductivity and permittivity) are critical for correct electromagnetic simulations and subsequent Specific Absorption Rate (SAR) assessment for various purposes, such as for safety assessment of Magnetic Resonance Imaging (MRI) [1,2] and telecommunications [3] or for thermal dose computation in Hyperthermia Treatment Planning (HTP) [4]. SAR is related to conductivity (σ) as $SAR = \sigma |E|^2 / (2\rho)$, where E is the electric field and ρ is the tissue density. Since many of the electric properties used in human models are based on *ex vivo* measurements of animal and human tissues [5,6], the accuracy of the *in vivo* SAR determination in specific applications may be questionable. Furthermore, a review of those measurements from many studies showed a large variation between the reported electrical properties [7]. These variations can be explained by the use of tissues of various species and variations in measuring conditions (tissue temperature, *in vivo*, *in vitro* and *ex vivo*). Based on this disparity, we believe that there is sufficient reason to verify the validity of the current maintained *in vivo* electric property values.

Due to practical and ethical reasons, human *in vivo* electric property measurements are scarce. Only easily accessible tissue types (e.g. skin, tongue) [5] and liver [8] have been measured *in vivo*. Therefore, MR based methods to measure electric properties non-invasively have recently received an increased attention. Electric Properties Tomography (EPT) [1,9–11] is such a non-invasive technique to reconstruct electric properties using B_1^+ field measurements acquired by standard MR techniques. EPT has

been previously applied for in vivo electric property reconstruction of human brain tissue [9,12,13] and liver [14,15]. In these studies good agreement was shown between the mean reconstructed values and probe measurements reported in the literature, and typically a standard deviation of around 20% is observed. As in general the conductivity value of tumors are elevated compared to healthy tissue, EPT is a potential tool for tumor characterization and has recently been utilized to reconstruct the conductivity values of gliomas [16,17] and breast tumors [18,19]. One of the limitations of EPT is the accuracy at tissue boundaries due to kernel based implementations and use of transceive phase assumption, therefore, various studies have investigated these issues [9,20–22].

In this work we utilize this technique to reconstruct the *in vivo* electric conductivity of tissues in the pelvic region. These results can be used for more accurate SAR determination in hyperthermia treatment planning of deeply seated pelvic tumors. Here, we report the conductivity of muscle, bladder and cervical tumor as reconstructed using EPT, based on measurements performed at 3T MRI. Finally, we compare those values to conductivity values reported in the literature for those tissue types.

4.2 Methods

In vivo MR measurements were conducted on 20 patients with cervical cancer in accordance with the approval of the Medical Ethics Board. 18 patients were histopathologically diagnosed with squamous-cell carcinoma (SCC) of the cervix, one was diagnosed with adenocarcinoma and one with endometrial carcinoma. Peristaltic bowel motion during the MRI scan was reduced with the intravenous injection of *Buscopan*® (Boehringer Ingelheim GmbH).

4.2.1 MR measurements

All experiments were conducted on a 3T MR system (Ingenia, Philips Healthcare, The Netherlands) using a 26 channel torso receive array. The B_1^+ amplitude map was acquired using the actual flip angle imaging (AFI) method [23] (3D, nom. flip angle = 65°, TR1/TR2=50/290ms, 2.5x2.5x5mm, 16 slices, scan duration ≈ 6 min.). The transceive phase was acquired by a spin echo (SE) sequence (TR=1200ms, 2.5x2.5x5mm, 16 slices, scan duration ≈ 6 min.) [24,25]. The receiver non-uniformity including the phase contribution of the receive array was eliminated by using the so-called CLEAR technique [26]. The net effect of this technique is that the phase of the receive array is replaced by the receive phase contribution of the system's birdcage body coil operated in reverse quadrature. To correct for eddy currents, the transceive phase was measured twice with opposing gradients [27]. Due to scan time limitations, a 5 mm isotropic resolution was used for 13 patients.

4.2.2. EPT reconstruction

The EPT reconstructions were performed using B_1^+ amplitude measurements and the transceive phase approximation ($\phi^+ \approx \phi^{\pm}/2$) was applied as described in literature [1,10,25,27].

Assuming that the dielectric properties are piece-wise constant, the tissue electric conductivity can be computed by the homogenous Helmholtz equation:

$$\frac{\nabla^2 B_1^+}{B_1^+} = -\mu_0 \varepsilon_0 \varepsilon_r \omega^2 - i\mu_0 \sigma \omega \tag{6}$$

where B_1^+ is the complex transmit field ($B_1^+ = |B_1^+|e^{i\phi^+}$), ε_r and σ are the relative permittivity and conductivity of the object of interest, respectively, ω is the Larmor angular frequency, and μ_0 and ε_0 are the permeability and permittivity of vacuum, respectively.

The conductivity can be computed by

$$\sigma = -\mathrm{Im}\left(\frac{\nabla^2 \left(\left| B_1^+ \right| e^{i\phi^+} \right)}{\left| B_1^+ \right| e^{i\phi^+}} \right) \frac{1}{\mu_0 \omega} = \frac{1}{\mu_0 \omega} \left(\nabla^2 \phi^+ + 2 \frac{\nabla \left| B_1^+ \right| \cdot \nabla \phi^+}{\left| B_1^+ \right|} \right) \tag{7}$$

where in the last part of Eq.(2), the identity $\nabla e^{i\phi^+} = e^{i\phi^+} i \nabla \phi^+$ was used [28].

The Laplacian required to evaluate Eq.(2) was computed by a kernel-based method as described in [27] using a kernel size of 7x7x5 voxels. This noise-robust kernel was used to reduce the effect of noise on the second derivative. The applied EPT method in this study was validated in a pelvic-sized phantom study in [11] where a good agreement was found between EPT based conductivity values and probe measurements (Model 85070C, HP/Agilent Corp, Santa Clara CA).

4.2.3 Quantification of in vivo data

The tumor volume was delineated by a radiation oncologist based on CT and T2-weighted MRI images (TR/TE=5906/80ms, 0.70x0.90x3.00 mm). *In vivo* MR measurements were used to reconstruct the electric conductivity and the reconstructed values were compared to literature values.

Average conductivity values were computed for all voxels inside a (manually) delineated volume-of-interest. All acquired slices have been used for the computations of the average and standard deviation of σ-values. To exclude the effect of boundary reconstruction errors related to EPT, the delineated regions excluded the boundaries where out-of-range σ-values were reconstructed. Furthermore, the first two pixels closest to the boundary were excluded and for a reliable reconstruction only tissues with a volume of at least 3.5x3.5x3.0cm^3 were considered. At the boundaries the

reconstructed values can be twice as high as the expected values and are therefore excluded by excluding the first two pixels closest to the boundary. As a consequence the bladder and tumor volume of only ten patients were sufficiently large to be included. All patients met the inclusion criteria for muscle tissue reconstructions. Computations regarding EPT reconstruction were performed using MATLAB® (The Mathworks, Natick, MA, U.S.).

4.3 Results

In Figure 1a and 1b, an example is depicted of the measured B_1^+ amplitude and transceive phase maps of a patient, respectively. The reconstructed σ-map based on Figures 1a and 1b is shown in Figure 1c. Figure 1c also shows the manual delineation of muscle tissue to exclude EPT-related boundary artifacts from the measurement. The T1-weighted image of the patient, acquired by the AFI sequence, is shown for anatomical reference in Figure 1d.

4.3.1 Muscle

In Figure 2 the electric conductivity (mean±std) of muscle of each patient is presented. The mean conductivity value of muscle found in this study is 0.93±0.26 S/m. In Figure 2 the literature value as given by Gabriel et al. [6] is also shown, a value widely used in human models for SAR assessment in various applications. The mean value found in this study is 14% higher than the value reported in [6]. In Figure 3 the distribution of the data of the 20 patients is presented along with the mean value and the value based on [6].

4.3.2 Bladder content/Urine

The reconstructed electric σ-values of bladder content of ten patients are presented in Figure 4. The interpatient variation is larger compared to muscle conductivity. The mean value based on this study is 1.76±0.42 S/m. The conductivity of urinary bladder wall tissue from the literature [5,29] is also shown, which is widely used for the whole bladder volume in human models [30–33]. Finally, the porcine urine conductivity value at 128MHz, based on [34], is also depicted in Figure 4.

4.3.3 Cervical tumor

In Figure 5 the reconstructed electric σ-values of tumor tissues are depicted. The σ-value of adenocarcinoma and endometrial carcinoma is slightly higher than for other tumor tissues. The conductivity of cervical tissue at 128MHz as reported in [6] is also shown in Figure 5. The mean value of all cervical tumors is 1.02±0.29 S/m which is 13% higher than the σ-value reported in [6].

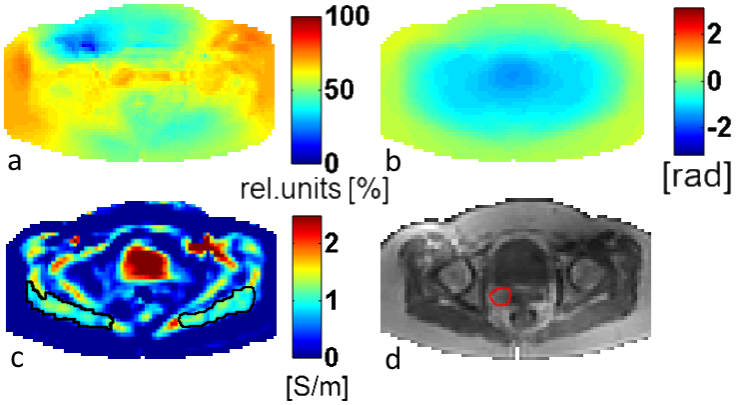

Figure 1. B_1^+ amplitude (a) and the transceive phase (b) of a patient. The reconstructed conductivity map (c) based on (a,b) and the corresponding T1 weighted image (d) acquired during the AFI sequence. The muscle delineation shown in black (c) excludes the EPT related boundary artifacts. The outline of the tumor is shown in red (d).

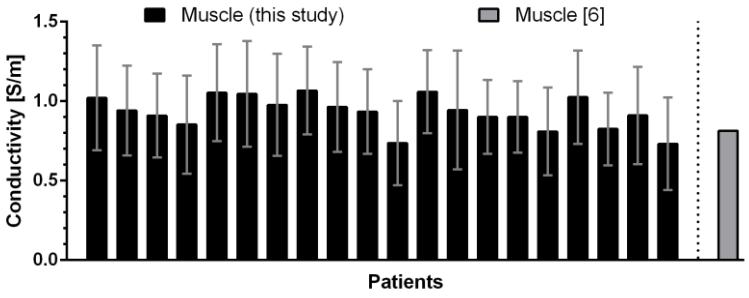

Figure 2. Muscle conductivity (mean±std) of each patient and the literature value based on [6] at 128 MHz.

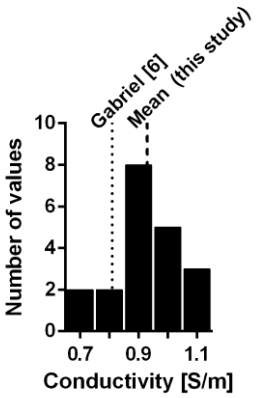

Figure 3. Distribution of the muscle data of 20 patients.

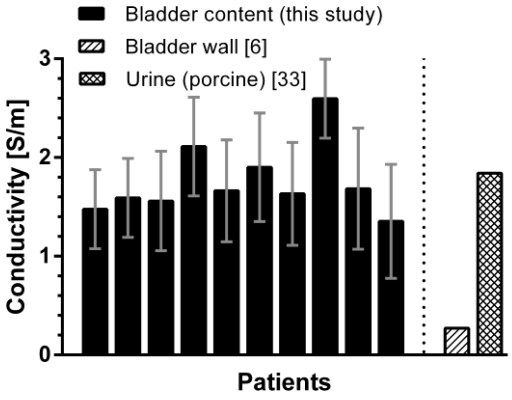

Figure 4. Bladder content conductivity based on this study and the literature value [6] based on bladder wall tissue. The last bar represents the conductivity value of porcine urine reported in [34].

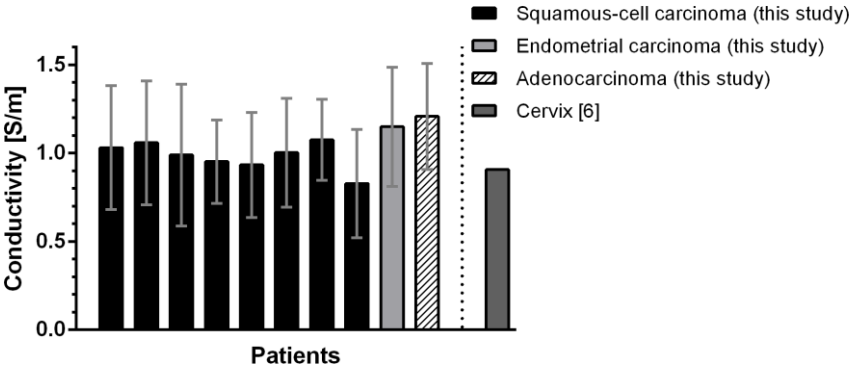

Figure 5. Cervical tumor σ-values observed in this study for squamous-cell carcinoma, adenocarcinoma and endometrial carcinoma compared to literature value.

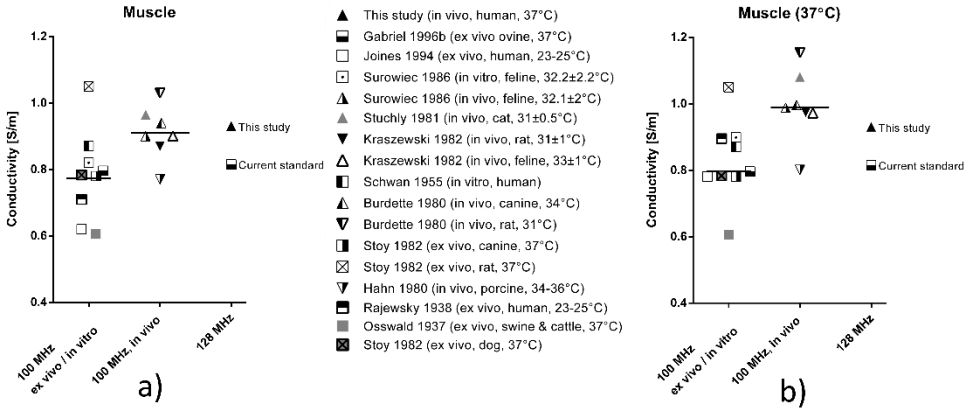

Figure 6. a) An overview of the available literature data at 100MHz and 128MHz for the conductivity of muscle along with the mean value based on this study. b) The literature data extrapolated to 37ºC by adjusting the conductivity values by 2%/ ºC. The horizontal line represents the median values of the *ex vivo/in vitro* data or the *in vivo* data.

4.4 Discussion

We have presented *in vivo* electrical σ-values as reconstructed by the EPT method based on B_1^+ data. The presented values correspond to σ-values at 128MHz as this is the Larmor frequency of a 3T MR system.

Since current implementations of EPT might show error artefacts at tissue boundaries, these regions have been excluded from the calculation of the mean conductivity. However, the performance of EPT of relatively large tissue regions is reliable as was demonstrated in pelvic-sized phantom experiments in [11] and brain studies [9,10,25]. Furthermore, we applied the transceive phase approximation, which was shown to hold for the pelvis anatomy in [11]. The standard deviation observed in this study and generally observed in EPT *in vivo* studies is due to the numerical implementation of the method and the heterogeneity of biological tissue. For instance, derivative operators act on typically noisy B1 data which together with the transceive phase approximation introduce around 20% standard deviation within a sample volume.

Various studies have focussed on clinical implementation of new approaches increasing the accuracy by using multi transmit channel systems or avoiding derivative operators [9,20,35,36]. However, the close agreement between the reconstructed values of 20 patients included in this study demonstrates the high reproducibility of the reconstructed conductivity values. Furthermore, we had repeat measurements available for three patients as they underwent a follow up MR scan after the treatment. The mean reconstructed muscle conductivity values in these three cases deviated less than 5% from the initially reconstructed conductivity values confirming the high reproducibility.

In general EPT is able to reconstruct the permittivity values as well. However, the reconstruction accuracy varies with field strength as shown earlier by van Lier et.al [12]. It was shown that the permittivity reconstruction in vivo is most accurate at 7T. Due to the limited accuracy of permittivity reconstruction at 3T we have focused on conductivity reconstruction only, since the acquisition of the latter contributes more substantially to more accurate SAR assessment. This was shown by Restivo et.al. [37] for tumor SAR assessment at 7T MRI and in deep hyperthermia studies in [4,38–40].

Currently, most electric property values presented in overviews like Gabriel et al. [7] are measured under different measurement conditions, hence report a large variance in values. We have compared σ-values reported in this study to the ones reported in the literature for the relevant frequency range, and included literature data available from animal studies at around body temperatures and human data at any temperature measured *in vivo, in vitro* or *ex vivo*.

Literature data are mostly presented in tables at distinct frequencies or in graphs. The latter necessitate estimation of σ-values at intermediate frequencies by interpolation. We have chosen to consider only studies which presented data for muscle tissue at 100MHz. In addition, we have included literature data at 128MHz (ie. Larmor frequency for 3T proton MRI imaging) if this was explicitly given or if Cole-Cole parameters were reported allowing computation of the value at 128MHz. In general, frequency dependence of tissue conductivity can be described by a Cole-Cole equation [41].

4.4.1 Muscle

Comparison of our measured values to values in the literature is challenging as conductivity measurements of human muscle are reported in just two studies [42] [43]. In [42], measurements were performed between 1 and 2 hours after excision at a temperature between 23-25°C. No information regarding measuring conditions is provided in [43]. Note that the currently used conductivity value for muscle, based on [6], is of ovine origin, measured *ex vivo* (at 37°C), and within 2h after the animal is sacrificed. A larger overview of literature data for muscle tissue of different species and obtained both *in vivo* and *ex vivo* is depicted in Figure 6a. In Figure 6a we have depicted the median of the reported σ-values in [44–46]. All other values shown in Figure 6a are mean values as reported in the corresponding studies [47–51]. In Figure 6b the temperature dependency of conductivity values is taken into account, therefore, the values of Figure 6a are extrapolated to 37ºC by adjusting the values with 2%/ºC as reported in [52,53]. The mean value found in this study is depicted alongside literature values and appears to be in good agreement with the *in vivo* values reported in the literature for different species.

Thus, based on σ-values reconstructed in this work, it is observed that the mean conductivity value of all patients is approximately 14% higher than the value reported in [6]. These findings are in agreement with the animal studies presenting *in vivo* σ-values as shown in Figure 6. We therefore reason that the currently used value for muscle conductivity slightly underestimates the true *in vivo* conductivity value, however, the

reported value in [6] falls within the uncertainty range of data presented in this study. Explanation for this 14% difference might be the higher blood and water content in living conditions. In [54] and [55] the effect on conductivity change after sacrifice was investigated for canine and porcine brain tissue, respectively, and a 15% conductivity decrease in the first 15 minutes after sacrifice was observed. Additionally, physiological difference between human and ovine muscle tissue may explain the difference between the literature values and the values observed in this study. We have, furthermore, noticed that the conductivity value reported for muscle in the table in [6] is around 14% higher than reported in the online databases [29,56]. We assume this discrepancy is introduced due to the use of Cole-Cole parameters in the latter databases which might lead to a mismatch at some frequencies compared to the true measurements [6] on which these Cole-Cole parameters are derived from.

Furthermore, [57] reported a decrease of conductivity with age for various rat tissues, including muscle, in a frequency range of 130MHz to 10GHz, attributed to changes in cell sizes, structure, water content and the ratio of free to bound water. Based on the Cole-Cole parameters presented in [57,58], the estimated σ-values at 130MHz of a new born and 70 days old rat muscle are 1.46 S/m and 0.68 S/m, respectively. In our study the patient age ranged between 30 and 86 years old, however, no significant age related conductivity differences were observed in the relatively small patient population included in the study.

4.3.2 Bladder content/Urine

There is a large discrepancy of an order of magnitude between the often used conductivity for bladder volume in human models [30–33] and *in vivo* reconstructed conductivity based on EPT (Figure 4). No study reports human urine σ-values at 128MHz, but one study [34] reports σ-values of porcine urine using samples of 21 animals (at 37°C). These yield, based on the reported Cole-Cole fitting parameters, a conductivity value of urine of 1.84 S/m at 128MHz, which is in good agreement with the human values found in this study (Figure 5). The reported root-mean-square-error of the fits was large [34], indicating a relatively large spread among samples. The results of the porcine study [34] were recently included in the online database [56], however, various SAR studies have been using the low conductivity value of bladder wall tissue for the whole bladder. There is one study reporting that human urine conductivity at 90 MHz is 1.81[S/m] [59] measured by an impedance probe (Model 85070C, HP/Agilent Corp, Santa Clara CA) which is in good agreement with our findings.

4.3.3. Cervical tumor

The only available data on human cervical tissue at 128MHz are found in [6] which is based on measurements (at 37°C) on excised non-specified (healthy or tumor) cervical tissue. The reported σ-value is 0.91 S/m. In contrast, the cervix conductivity value used in, for instance, Virtual Family models [56] and in the online available database [29] is

much lower: 0.75 S/m (at 128MHz). The σ-value at 128MHz based on [6] is shown in Figure 5.

To the best of our knowledge, no data are available regarding cervical tumor σ-values at 128MHz. The only reports on cervical tumor conductivity are based on measurements at 4.8 kHz and 614 kHz [60], where no significant difference in average σ-values were observed between healthy and pathological cervix uteri. However, Trokhanova *et al* [60] did observe a higher electrical conductivity value within the zone of the external fauces.

The average conductivity found in cervical tumors in this study is approximately 13% higher compared to [6]. In our study however, we have not reconstructed the conductivity of healthy cervical tissue for comparison. We therefore have insufficient evidence to expect that our EPT technique is capable of differentiating this particular tumor type. We do not exclude of course that this technique is capable of differentiating other types of pelvic tumors provided the tumor is large enough and provided that this tumor type has conductivity properties which deviate more significantly from the surrounding normal tissue as was the case for the breast tumors evaluated by Katscher et al. [18]. A further comparison between healthy and diseased cervical tissue is warranted to enable interpretation of the observed differences.

4.5 Conclusion

This study indicates that the human *in vivo* electric conductivity values appear to deviate slightly from values provided in the present databases at the investigated frequency and conductivity values should therefore be evaluated in a larger *in vivo* study investigating more human tissues. The *in vivo* values reported in this study were in good agreement with available *in vivo* data from the literature. The presented results have an impact on power absorption computations, used among others for hyperthermia treatment planning, emphasizing the importance of using *in vivo* values when incorporating electric conductivity data into numerical models.

Acknowledgments

This study was supported by grant UVA 2010-4660 of the Dutch Cancer Society.

References

[1] Katscher U, Voigt T, Findeklee C, Vernickel P, Nehrke K, Dössel O. Determination of electric conductivity and local SAR via B1 mapping. *IEEE Trans Med Imaging* 2009;28:1365–74.

[2] Zhang X, Schmitter S, Van de Moortele P-F, Liu J, He B. From complex B(1) mapping to local SAR estimation for human brain MR imaging using multi-channel transceiver coil at 7T. *IEEE Trans Med Imaging* 2013;32:1058–67.

[3] Peyman A, Gabriel C, Grant EH, Vermeeren G, Martens L. Variation of the dielectric properties of tissues with age: the effect on the values of SAR in children when exposed to walkie-talkie devices. *Phys Med Biol* 2009;54:227–41.

[4] de Greef M, Kok HP, Correia D, Borsboom P-P, Bel A, Crezee J. Uncertainty in

hyperthermia treatment planning: the need for robust system design. *Phys Med Biol* 2011;56:3233–50.

[5] Gabriel S, Lau RW, Gabriel C. The dielectric properties of biological tissues : II . Measurements in the frequency range 10 Hz to 20 GHz. *Phys Med Biol* 1996;41:2251–69.

[6] Gabriel C. Compilation of the Dielectric Properties of Body Tissues at RF and Microwave Frequencies. Brooks Air Force Tech Rep 1996;AL/OE-TR:0037.

[7] Gabriel C, Gabriel S, Corthout E. The dielectric properties of biological tissues: I. Literature survey. *Phys Med Biol* 1996;41:2231–49.

[8] O'Rourke AP, Lazebnik M, Bertram JM, Converse MC, Hagness SC, Webster JG, et al. Dielectric properties of human normal, malignant and cirrhotic liver tissue: in vivo and ex vivo measurements from 0.5 to 20 GHz using a precision open-ended coaxial probe. *Phys Med Biol* 2007;52:4707–19.

[9] Liu J, Zhang X, Schmitter S, Van de Moortele P-F, He B. Gradient-based electrical properties tomography (gEPT): A robust method for mapping electrical properties of biological tissues in vivo using magnetic resonance imaging. *Magn Reson Med* 2015;74:634–46.

[10] van Lier ALHMW, Raaijmakers A, Voigt T, Lagendijk JJW, Luijten PR, Katscher U, et al. Electrical Properties Tomography in the Human Brain at 1.5, 3, and 7T: A Comparison Study. *Magn Reson Med* 2013;000:354–63.

[11] Balidemaj E, Van Lier ALHMW, Crezee H, Nederveen AJ, Stalpers LJA, Van Den Berg CAT. Feasibility of electric property tomography of pelvic tumors at 3T. *Magn Reson Med* 2014;73:1505–13.

[12] Van Lier ALHMW, Raaijmakers A, Voigt T, Lagendijk JJW, Luijten PR, Katscher U, et al. Electrical Properties Tomography in the Human Brain at 1 . 5 , 3 , and 7T : A Comparison Study. *Magn Reson Med* 2013.

[13] Voigt T, Katscher U, Doessel O. Quantitative conductivity and permittivity imaging of the human brain using electric properties tomography. *Magn Reson Med* 2011;66:456–66.

[14] Stehning C, Voigt T, Karkowski P, Katscher U. Electric Properties Tomography (EPT) of the Liver in a Single Breathhold Using SSFP. *Proc 20th Annu Meet ISMRM* 2012:386.

[15] Kim M-O, Choi N, Shin J, Lee J, Kim1 D-H. Phase unbanding in bSSFP for Liver conductivity imaging at 3.0T. *Proc 21th Annu Meet ISMRM* 2013:4173.

[16] Voigt T, Väterlein O, Stehning C, Katscher U, Fiehler J. In vivo Glioma Characterization using MR Conductivity Imaging. *Proc 19th Annu Meet ISMRM* 2011;19:2865.

[17] van Lier AL, Hoogduin JM, Polders DL, Boer VO, Hendrikse J, Robe PA, et al. Electrical conductivity imaging of brain tumours. *Proc 19th Annu Meet ISMRM* 2011;19:4464.

[18] Katscher U, Abe H, Ivancevic M, Djamshidi K, Karkowski P, Newstead G. Towards the investigation of breast tumor malignancy via electric conductivity measurement. *Proc 21th Annu Meet ISMRM* 2013;21:3372.

[19] Shin J, Kim MJ, Lee J, Nam Y, Kim M, Choi N, et al. Initial study on in vivo conductivity mapping of breast cancer using MRI. *J Magn Reson Imaging* 2014;42:371–8.

[20] Balidemaj E, van den Berg CAT, Trinks J, Lier A van, Nederveen AN, Stalpers LJA, et al. CSI-EPT: A Contrast Source Inversion Approach for Improved MRI-Based Electric Properties Tomography. *IEEE Trans Med Imaging* 2015;34:1788–96.
[21] Sodickson DK, Alon L, Deniz CM, Ben-Eliezer N, Cloos M, Sodickson LA, et al. Generalized Local Maxwell Tomography for Mapping of Electrical Property Gradients and Tensors. *Proc 21th Annu Meet* 2013:4175.
[22] Hafalir FS, Oran OF, Gurler N, Ider YZ. Convection-reaction equation based magnetic resonance electrical properties tomography (cr-MREPT). *IEEE Trans Med Imaging* 2014;33:777–93.
[23] Yarnykh VL. Actual flip-angle imaging in the pulsed steady state: a method for rapid three-dimensional mapping of the transmitted radiofrequency field. *Magn Reson Med* 2007;57:192–200.
[24] van Lier ALHMW, van den Berg CAT, Katscher U. Measuring electrical conductivity at low frequency using the eddy currents induced by the imaging gradients. *Proc 20th Annu Meet ISMRM* 2012:3467.
[25] Voigt T, Katscher U, Doessel O. Quantitative conductivity and permittivity imaging of the human brain using electric properties tomography. *Magn Reson Med* 2011;66:456–66.
[26] Voigt T, Homann H, Katscher U, Doessel O. Patient-individual local SAR determination: in vivo measurements and numerical validation. *Magn Reson Med* 2012;68:1117–26.
[27] van Lier ALHMW, Brunner DO, Pruessmann KP, Klomp DWJ, Luijten PR, Lagendijk JJW, et al. B1(+) phase mapping at 7 T and its application for in vivo electrical conductivity mapping. *Magn Reson Med* 2012;67:552–61.
[28] van Lier ALHMW. Electromagnetic and Thermal Aspects of Radiofrequency Field Propagation in Ultra-High Field MRI. PhD Dissertation; 2012.
[29] Andreuccetti D, Fossi R, Petrucci C. An Internet resource for the calculation of the dielectric properties of body tissues in the frequency range 10 Hz - 100 GHz. Website at http://niremf.ifac.cnr.it/tissprop/. IFAC-CNR, Florence (Italy), 1997.
[30] Fenn AJ. Adaptive Phased Array Thermotherapy for Cancer. 1st ed. Artech House, pp.70; 2008.
[31] Saunders SR, Aragon Zavala A. Antennas and Propagation for Wireless Communication Systems. 2nd ed. John Wiley & Sons, Ltd; 2007.
[32] Homann H. SAR Prediction and SAR Management for Parallel Transmit MRI. PhD Dissertation; 2012.
[33] Amjad A. Specific absorption rate during magnetic resonance imaging. PhD Dissertation; 2007.
[34] Peyman A, Gabriel C. Dielectric properties of porcine glands, gonads and body fluids. *Phys Med Biol* 2012;57:N339–44.
[35] Marques JP, Sodickson DK, Ipek O, Collins CM, Gruetter R. Single acquisition electrical property mapping based on relative coil sensitivities: A proof-of-concept demonstration. *Magn Reson Med* 2014;00:1–11.
[36] Liu J, Zhang X, Van de Moortele P-F, Schmitter S, He B. Determining electrical properties based on B1 fields measured in an MR scanner using a multi-channel transmit/receive coil: a general approach. *Phys Med Biol* 2013;58:4395–408.
[37] Restivo MC, van den Berg CAT, van Lier ALHM., Polders DL, Raaijmakers AJE,

Luijten PR, et al. Local specific absorption rate in brain tumors at 7 Tesla. *Magn Reson Med* 2015;75(1):381-9.

[38] Kamer JB Van De, Wieringen N Van, LeeuwA A C De, Lagendijk JJW. The significance of accurate dielectric tissue data for hyperthermia. *Int J Hyperth* 2001;17:123–42.

[39] Canters RAM, Paulides MM, Franckena M, Mens JW, van Rhoon GC. Benefit of replacing the Sigma-60 by the Sigma-Eye applicator. A Monte Carlo-based uncertainty analysis. *Strahlentherapie Und Onkol* 2013;189:74–80.

[40] Balidemaj E, Kok HP, Schooneveldt G, Lier ALHMW, Remis RF, Stalpers LJA, et al. Hyperthermia Treatment Planning for cervical cancer patients based on electric conductivity tissue properties acquired in vivo from B1+ maps with EPT at 3T MRI. *Int J Hyperth* 2015;in press.

[41] Cole KS, Cole RH. Dispersion and Absorption in Dielectrics I. Alternating Current Characteristics. *J Chem Phys* 1941;9:341.

[42] Joines WT, Zhang Y, Li C JR. The measured electrical properties of normal and malignant human tissues from 50 to 900 MHz. *Med Phys* Phys 1994;21:547–50.

[43] Schwan HP. Application of uhf impedance measuring techniques in biophysics. *IRE Trans Med Eletron* 1955;PGME-4:75.

[44] Stuchly MA, Athey TW, Stuchly SS, Samaras GM, Taylor G. Dielectric properties of animal in vivo at frequencies 10 MHz - 1GHz. *Bioelectromagnetics* 1981;2:93–103.

[45] Stoy RD, Foster KR, Schwant HP. Dielectric properties of mammalian tissues from 0.1 to l00 MHz: a summary of recent data. *Phys Med Biol* 1982;27:501–13.

[46] Osswald K. Messung der Leitfahigkeit und Dielektrizitatkonstante biologischer Gewebe und Flussigkeiten bei kurzen Wellen. *Hochfrequenz Tech Elektroakustik* 1937;49:40–50.

[47] Surowiect A, Stuchlyt SS, Keaneys M, Swarup A. In vivo and in vitro dielectric properties of feline tissues at low radiofrequencies. *Phys Med Biol* 1986;31:901–9.

[48] Kraszewski A, Stuchly MA, Stuchly SS, Smith A. In vivo and in vtiro dielectric properties of animal tissues at radio frequencies. *Bioelectromagnetics* 1982;3:421–32.

[49] Hahn GM, Kernahan P, Martinez A, Pounds D, Prionas S, Anderson T, et al. Some heat transfer problems associated with heating by ultrasound, microwaves, or radio frequency. Ann New York Acad Sci 1980;335:327–51.

[50] Burdette EC, Cain FL, Seals J. In Vivo Probe Measurement Technique for Determining Dielectric Properties at VHF Through Microwave Frequencies. *IEEE Trans Microw Theory Tech* 1980;MTT-28:414–27.

[51] Rajewski B. Ultrakurzwellen, Ergebnisse der biophysikalishen Forschung. Bd 1. (Leipzig: Georg Thieme); 1938.

[52] Stogryn A. Equations for calculating the dielectric constant of saline water. *IEEE Trans Microw Theory Tech* 1971;19:733–6.

[53] Leussler C, Karkowski P, Katscher U. Tempendent-dependent Conductivity Change using MR-based Electric Properties Tomography. *Proc 20th Annu Meet ISMRM* 2012:3451.

[54] Burdette EC, Friederich PG, Seaman RL, Larsen LE. In Situ Permittivity of Canine Brain: Regional Variations and Postmortem Changes. *IEEE Trans Microw Theory Tech* 1986;34:38–50.

[55] Schmid G, Neubauer G, Illievich UM. Dielectric Properties of Porcine BrainTissue in

theTransition From Life to Death at Frequencies From 800 to 1900 MHz. *Bioelectromagnetics* 2003;24:413–22.

[56] Hasgall P, Di Gennaro F, Baumgartner C, Neufeld E, Gosselin M, Payne D, et al. IT'IS Database for thermal and electromagnetic parameters of biological tissues," Version 2.6, January 13th, 2015. www.itis.ethz.ch/database n.d.

[57] Peyman A, Rezazadeh A A and Gabriel C. Changes in the dielectric properties of rat tissue as a function of age at microwave frequencies. *Phys Med Biol* 2001;46:1617–29.

[58] Peyman A, Rezazadeh AA, C. Gabriel. Corrigendum: Changes in the dielectric properties of rat tissue as a function of age at microwave frequencies *Phys Med Biol* 2002;47:2187–8.

[59] Yuan Y, Cheng K-S, Craciunescu OI, Stauffer PR, Maccarini PF, Arunachalam K, et al. Utility of treatment planning for thermochemotherapy treatment of nonmuscle invasive bladder carcinoma. *Med Phys* 2012;39:1170–81.

[60] Trokhanova OV, Chijova YA, Okhapkin MB, Korjenevsky AV, Tuykin TS. Using of electrical impedance tomography for diagnostics of the cervix uteri diseases. *J Phys Conf Ser* 2010;224.